Rapid Identification of Metal-Binding Peptoid Oligomers by On-Resin X-Ray Fluorescence Screening

Danielle M. Nalband,[1] Benjamin P. Warner,[2] Nathan H. Zahler,[2] Kent Kirshenbaum[1]
[1]*Department of Chemistry, New York University, New York, NY 10003*
[2]*XRpro Corp, One Kendall Square, STE B2002, Cambridge, MA 02139*

Received 29 April 2014; revised 17 July 2014; accepted 18 July 2014
Published online 24 July 2014 in Wiley Online Library (wileyonlinelibrary.com). DOI 10.1002/bip.22528

ABSTRACT:

N-Substituted glycine peptoid oligomers have recently attracted attention for their metal binding capabilities. Due to their efficient synthesis on solid phase, peptoids are well suited for generation of compound libraries, followed by screening for molecular recognition and other diverse functional attributes. Ideally, peptoids could be simultaneously screened for binding to a number of metal species. Here, we demonstrate the use of bench-top X-ray fluorescence (XRF) instrumentation to screen rapidly, on solid support, a library of peptoid oligomers incorporating metal-binding functionalities. A subset of the peptoid sequences exhibited significant metal binding capabilities, including a peptoid pentamer and a nonamer that were shown to selectively bind nickel. The binding capabilities were validated by colorimetric assay and by depletion of Ni^{2+} ion concentration from solution, establishing bench-top XRF as a rapid, practicable high-throughput screening technique for peptoid oligomers. This protocol will facilitate discovery of metallopeptoids with unique material properties. © *2014 Wiley Periodicals, Inc. Biopolymers (Pept Sci) 102: 407–415, 2014.*

Keywords: foldamers; metallopeptoids; one bead one compound; combinatorial screening; transition metal

This article was originally published online as an accepted preprint. The "Published Online" date corresponds to the preprint version. You can request a copy of any preprints from the past two calendar years by emailing the Biopolymers editorial office at biopolymers@wiley.com.

INTRODUCTION

N-Substituted glycine oligomers, termed peptoids, are a class of sequence-specific oligomers that exhibit a range of biomimetic structural and functional attributes.[1] Peptoids can be readily assembled via a robust solid-phase synthesis protocol to incorporate a wide variety of side chain functional groups.[2] Early studies of peptoid oligomers demonstrated the ability to generate large combinatorial libraries suitable for high-throughput screening.[3] These efforts were primarily devoted to the identification of short oligomers to address challenges in small molecule drug discovery.[3–5] In 1994, the Zuckermann group reported peptoid trimers that antagonize protein receptors, which were among the first reports to screen large combinatorial libraries on-resin to identify oligomers targeting proteins of biomedical importance.[3]

Subsequently, peptoid synthesis protocols have been elaborated to attain substantial oligomer chain lengths, enabling the extension of these screening efforts to more advanced biomedical and materials applications.[6] Peptoid oligomer libraries have expanded in size (with some exceeding 250,000 compounds), and the therapeutic potential of peptoid sequences identified from screening operations has been established through in vitro and in vivo studies.[3,5,7,8] Split and pool synthesis techniques have been developed for generating diverse one bead one compound (OBOC) libraries, followed by sequence deconvolution of hit compounds by mass spectrometry.[9]

Additional Supporting Information may be found in the online version of this article.

Correspondence to: Kent Kirshenbaum; e-mail: kent@nyu.edu

Contract grant sponsor: NSF
Contract grant number: Award CHE-1152317

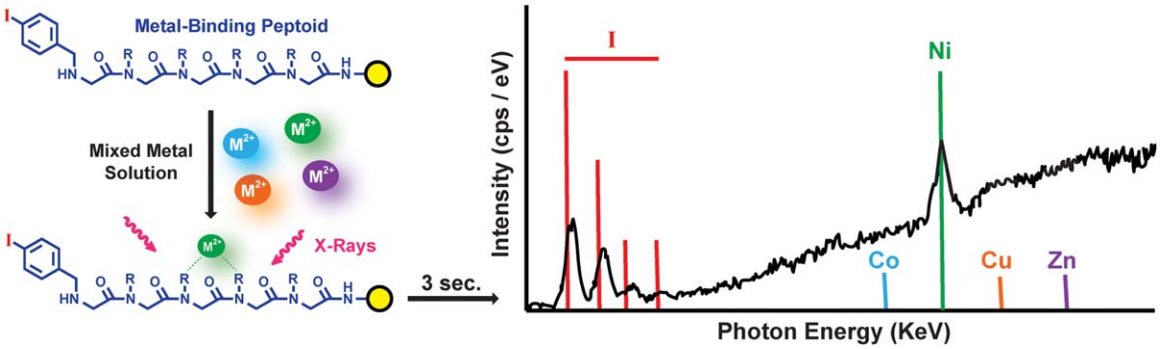

FIGURE 1 Schematic representation of screening one bead one compound peptoid oligomer libraries for metal binding using X-ray fluorescence. Following incubation in a solution of mixed divalent metal species, oligomer library members are subjected to 3 sec of X-ray irradiation, and spectra are acquired. The iodine signal confirms the presence of peptoid on resin, and binders are identified by the distinct atomic emission lines presented by each metal species. Here, the large nickel signal above the background noise indicates a nickel-binding interaction.

The incorporation of chemical diversity within conformationally ordered peptoid oligomers has also been investigated to focus on biomedical and materials objectives.[10–19] For example, the precise display of chemical functional groups along the oligomer backbone provides control over the crystallization of inorganic species and can also be used to establish selective catalysis.[14,20] Additional functional attributes may be attained through the coordination of metallic species to the oligomer framework.[21–29] Previous reports have determined that peptoid secondary structure can be modulated upon metal binding.[22–24] Recently, a conformationally ordered peptoid macrocycle was shown to coordinate Gd^{3+}, establishing favorable magnetic resonance relaxometric properties.[27] Moreover, peptoids displaying sulfhydryl functional groups can be used to deplete chromium (VI) from solution.[28]

Ideally, additional studies of "metallopeptoid" structures and functions could be enabled through screening efforts. While numerous precedents have described screening techniques to identify metal–biopolymer interactions on solid phase, most rely on colorimetric assays and are limited to the analysis of one metal per screen.[25,28,30] These requirements may impede the efficient discovery of peptoids capable of selective metal ion complexation.

Recent advances make X-ray fluorescence (XRF) an attractive technology for assaying the ability of peptoids to bind specific metal ions. XRF is a versatile technique, commonly used in materials science for quantifying the elemental composition of samples. For XRF, samples are illuminated with an X-ray source with photons sufficiently energetic to eject an electron from a 1s or 2s orbital.[31] Subsequent electron transitions that fill the resulting vacancy emit photons with energies in the X-ray regime. The XRF emission lines of each chemical element are distinct and can be quantified simultaneously, allowing unambiguous analysis of complexation or removal of a chemical species from a host.[31,32] Because XRF electron transitions involve inner electron orbitals, XRF is independent of the chemical form of the elements measured. When quantifying binding events, XRF is simply dependent on the presence and quantity of the atom of interest, and is independent of chemical form (e.g., oxidation state, ligands) or type of binding (e.g., covalent, noncovalent). In addition, XRF eliminates many matrix effects, as complex solutions and background are largely transparent for photons in this energy range.

Here, we demonstrate the use of a new bench-top micro XRF high-throughput screening process (XRpro MXRF®) for quantifying the metal binding characteristics of peptoid libraries (Figure 1). MXRF® analysis can be carried out with nanogram-sized samples and has detection limits between 20 and 100 pmol, enabling analysis of "one-bead-one-compound" libraries of oligomers immobilized on solid support for selective metal binding.[33] The analysis is non-destructive and is conducted in seconds per sample, allowing for the screening of large libraries in short amount of time. We employ MXRF® to screen a small library of peptoid oligomers on resin for metal binding interactions and identify peptoid sequences that preferentially bind Ni^{2+} from a solution of competing divalent transition metal species.

METHODS AND MATERIALS

Materials

Synthesis of the peptoid oligomers was initiated on either Rink Amide resin (Nova Biochem, 100–200 mesh, loading: 0.74 mmol/g) or NovaSyn TG amino resin HL (Nova Biochem, 110 μm, loading: 0.39 mmol/g). Bromoacetic acid (97%) was supplied by Sigma-Aldrich. Chloroacetic acid (99%),

trifluoroacetic acid, TFA, (99%), *N,N*-dimethylformamide, DMF, (anhydrous and amine free, 99.9%), and *N,N′* diisopropylcarbodiimide, DIC, (99%) were supplied by Alpha Aesar. Metal salts were obtained from the following sources: $Cu(NO_3)_2$•$3H_2O$ (Acros Organics, 99%), $Co(NO_3)_2$•$6H_2O$ (Alpha Aesar, 98–102%), $Ni(NO_3)_2$•$6H_2O$ (98%, Alpha Aesar), $Zn(NO_3)_2$•$6H_2O$ (Strem Chemicals, 98%). XRpro® analytical array plate seals were obtained from XRpro Corp, Cambridge, MA. Other reagents and solvents were obtained from commercial sources and used without additional purification.

Submonomers

The introduction of specific peptoid side chain types was achieved through the use of the following primary amines as "submonomer" synthons (see below):

Non-proteinogenic: 2-Methoxyethylamine (Sigma-Aldrich, 99%); butylamine (Sigma-Aldrich, 99.5%); (*S*)-(+)-1-cyclohexylethylamine (Alpha Aesar, 98%, 97% ee); (*S*)-(-)-1-phenylethylamine (TCI America, 98%); benzylamine (Alpha Aesar, 98%); 4-iodobenzylamine (Alpha Aesar, 97%); 4-(aminomethyl) pyridine (Sigma-Aldrich, 98%).

Proteinogenic: Ethanolamine (Sigma-Aldrich, 99%); histamine (CalbioChem, Free base, 97%); tyramine (TCI America, 98%); tryptamine (Sigma-Aldrich, 98%); and H-β-alanine-OtBu•HCl (NovaBiochem).

Instrumentation

Peptoid oligomers were analyzed by reverse-phase HPLC (analytical C_{18} column, Peeke Scientific, 5 mm, 120 Angstroms, 2.0 × 50 mm) on a Beckman Coulter Systems Gold 166 instrument. A linear gradient of 5–95% acetonitrile in water (0.1% TFA) over 10 min was used at a flow rate of 700 μL /min. Semi-preparative HPLC was performed using a Delta-Pak C_{18} column (Waters, 15 mm, 100 Angstroms, 25 × 100 mm). Peaks were eluted with a linear gradient of acetonitrile/water (0.1% TFA) which depended on the sequence composition with a flow rate of 2.5 mL/min. Mass spectrometry was performed on an Agilent 1100 series. XRF measurements were performed using an XRpro® micro XRF system equipped with a 30 W Rh excitation source, silicon drift energy-resolving detector, and having a 100 μm nominal X-ray spot size. X-ray tube operating conditions were maintained at 35 kV and 600 mA. Single resin beads were analyzed using XRpro® analytical array plate seals (XRpro Corp., Cambridge MA). Each XRpro® plate seal (127.8 mm × 85.5 mm) was divided into 48 sections (2 wells/section on a standard 96-well plate). In each section, identical sequences were immobilized, such that each sequence was positioned into two different, adjacent wells. For the nickel dimethylglyoxime assay, the four sequences were immobilized on a XRpro® analytical array plate seal (127.8 mm × 85.5 mm) such that each sequence was positioned into 12 different wells. The beads were visualized using a Zeiss Axioscope 40 Microscope with a halogen lamp, and images were captured using a Nikon D80 camera with an exposure time of 1/40 sec. Quantitation of Nickel concentration was performed by inductively coupled plasma mass spectrometry (ICP-MS) at a contract facility.

Preparation of Peptoid Oligomers on Tentagel Amino HL Resin. Peptoid oligomers were synthesized according to a modified submonomer approach.[2(b),34] The resin (10 mg, 0.0039 mmol reactive groups) was swelled for 1 h in DMF before initiating the synthesis. Bromoacetylation was carried out by incubating the resin with a bromoacetic acid solution in DMF (1.2*M*, 300 μL) and DIC (60 μL) for 40 min at 37°C and an agitation rate of 220 rpm. The resin was washed with 4 × 1 mL DMF before displacement with the desired primary amine (1*M* in DMF or 2*M* in NMP for heterocyclic amines and 4-iodobenzylamine, 300 μL) for 1 h at 37°C and an agitation rate of 220 rpm. The resin was washed with 5 × 1 mL DMF. For all steps subsequent to the addition of a heterocyclic amine, the iterative protocol was changed to acylation with chloroacetic acid solution in DMF (0.4*M*, 300 μL) with DIC (60 μL) for 10 min at 37°C and an agitation rate of 220 rpm. The washing and amine displacement steps were not modified. This two-step iterative process was repeated until the desired chain length and oligomer composition was achieved. Protecting groups were removed with a cocktail of 95% TFA, 2.5% TIPS, and 2.5% water (300 μL) at room temperature for 2 h. Resins were washed thoroughly with DCM, lyophilized, and stored under vacuum and desiccation until use.

Preparation of Peptoid Oligomers on Rink Amide Resin. Peptoid oligomers were synthesized according to a modified submonomer approach.[2(b),34] Rink Amide Resin, 100 mg (0.074 mmol), was swelled in DMF for 30 min before initiating the synthesis. Bromoacetylation was carried out by incubating the resin with a bromoacetic acid solution in DMF (1.2*M*, 850 μL) and DIC (200 μL) for 20 min at room temperature and an agitation rate of 220 rpm. The resin was washed with 4 × 1 mL DMF before displacement with the desired primary amine (1*M* in DMF or 2*M* in NMP for heterocyclic amines and 4-iodobenzylamine, 1 mL) for 30 min at room temperature and an agitation rate of 220 rpm. The resin was washed with 5 × 1 mL DMF. For all steps subsequent to the addition of a heterocyclic amine, the iterative protocol was changed to acylation with chloroacetic acid solution in DMF (0.4*M*, 850 μL) with DIC (200 μL) at 37°C for 10 min. Following a 4 × 1 mL DMF wash, displacement with the primary amine (1*M*

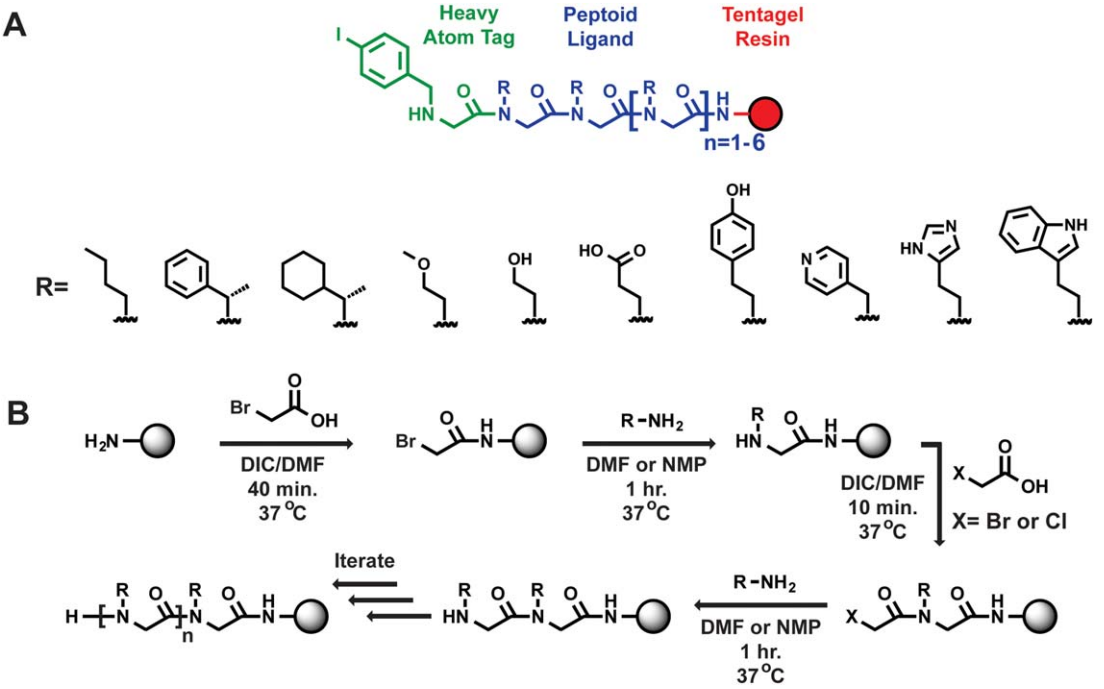

FIGURE 2 A: Peptoid oligomer library member. The members include the Tentagel resin incorporating a PEG linker (red), the peptoid oligomer with diverse side chain groups (blue), and a 4-iodobenzyl heavy atom tag, 4-iodobenzylamine, which was positioned at either the N or C terminus (green). The diversity of peptoid side chain groups incorporated into the library is shown below. B: Synthesis of peptoid library on Tentagel resin. Iterated steps include either bromoacetylation or chloroacetylation using DIC as a coupling agent, followed by displacement with a primary amine. Gray spheres represent the Tentagel resin bead.

or 2*M* for heterocyclic amines, 1 mL) was conducted at 37°C for 60 min. This two-step iterative process was repeated until the desired oligomer chain length and monomer sequence composition was achieved. The oligomers were cleaved from the resin using a cocktail containing 95% TFA, 2.5% TIPS, and 2.5% water (4 mL) at room temperature for 10 min. The solution was removed under reduced pressure, and the crude peptoid was re-suspended in acetonitrile/water, frozen, and lyophilized. Once thoroughly dried, crude peptoids were stored at 4°C until characterization and purification.

Incubation of Sequences Synthesized on Tentagel Resin With Metal Solution. Peptoid-functionalized Tentagel amino HL resin beads were positioned on an XRpro® analytical array plate seal as described above. The slide was affixed to a standard 96-well plate. Each well contained 3 mL of a 500 μ*M* stock solution of each of the following metals in water: $Cu(NO_3)_2 \cdot 3H_2O$, $Co(NO_3)_2 \cdot 6H_2O$, $Ni(NO_3)_2 \cdot 6H_2O$, $Zn(NO_3)_2 \cdot 6H_2O$ (pH of metal stock was adjusted to 7–8 with 1*M* Tris buffer pH 8 prior to partitioning solution into the wells). The sealed 96-well plate was inverted so that the solution was able to make contact with the resin-bound library. The library was incubated for 18–24 h in the metal solution prior to MXRF® analysis.

Dimethylglyoxime Colorimetric Analysis. Tentagel amino HL resin functionalized with peptoids (**ConC, PentA, NonaB**) and unmodified Tentagel amino HL resin beads (**ConTG**) were immobilized on an XRpro® analytical array plate seal as described above. The slide was affixed to a generic 96-well plate. Each well contained 3 mL of a 500 μ*M* solution of $Ni(NO_3)_2 \cdot 6H_2O$ in aqueous buffer (pH 7 adjusted with 0.5*M* Tris buffer pH 8 prior to exposure to beads). The sealed 96-well plate was inverted so that the nickel solution was able to make contact with the resin-bound peptoids. Following a 3 h incubation period in the nickel solution, the plate seal was removed, and the beads, which remained on the slide, were washed with 3 × 20 μL 0.5*M* Tris buffer. The beads were quickly dried with a stream of nitrogen before exposure to a 1% dimethylglyoxime solution in methanol (100 μL). Once the methanol had evaporated, all beads were viewed under a

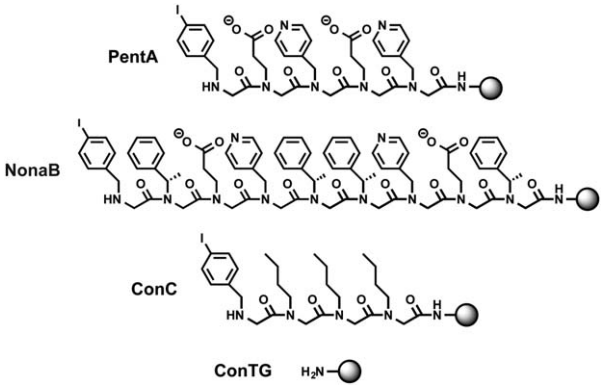

FIGURE 3 Chemical structures of peptoid hit compounds identified as nickel binders by Micro XRF: **PentA** and **NonaB**. Controls used in the study: **ConC** and unmodified Tentagel Beads (**ConTG**).

microscope, and a representative color image of each sequence, on resin, was obtained.

Nickel Depletion Assay. Each peptoid sequence, immobilized on resin, was weighed (5 mg, 1.95 μmol) and incubated with agitation for 3 h in either a 24.1$M \pm$ 1.8 $Ni(NO_3)_2$ (0.241 μmol, 10 mL) or a 222.5 μ$M \pm$ 22.8 $Ni(NO_3)_2$ (0.222.5 μmol, 1 mL) aqueous Tris-buffered solution (pH 7). The solutions were filtered to remove any resin beads and submitted for ICP-MS analysis of nickel concentration, along with samples of the starting nickel solutions.

RESULTS AND DISCUSSION

Design and Synthesis of the Peptoid Library

We designed a family of peptoid sequences bearing side chain functional groups that would enable metal complexation. The peptoid sequences included N-substituted glycine monomers that emulate proteinogenic side chains such as histidine, glutamic acid, tryptophan, serine, and tyrosine. We also took advantage of the extensive chemical diversity offered by peptoid solid-phase synthesis to include non-proteinogenic side chain groups, such as pyridylalanine (Figure 2A). In addition, we evaluated a negative control peptoid sequence, "**ConC**," composed solely of alkyl side chains, and thus not anticipated to exhibit significant inherent metal-binding capabilities. Unmodified Tentagel resin beads, referred to as "**ConTG**," were also subjected to analysis of metal binding.

To control for variations in the bead size and the amount of peptoid on single-bead samples, we incorporated a "reporter" monomer displaying an iodobenzyl group in the oligomer sequence designs at either the N- or C-terminus (Figure 2A). Iodine produces XRF emission lines similar in energy to those of the metals of interest (Cu, Co, Ni, and Zn), but sufficiently distinct in the spectrum so as not to interfere with their emission lines (see Supporting Information Figure S1). The presence and intensity of an iodine XRF signal could therefore be used to confirm the presence of the peptoid oligomers on resin and to enable ratiometric analysis of the metal to iodine signal. This ratio enables comparative evaluation of metal binding by different peptoid sequences.

Following the design, a library of 35 peptoid sequences (see Supporting Information Figure S2) was synthesized on NovaSyn TG amino resin HL according to a modified "submonomer" synthesis approach[2,34] at >80% purity (as determined by relative peak integration using reversed-phase high performance liquid chromatography) (Figure 2B, see Supporting Information Figure S3). This synthesis protocol entails an iteration of sequential haloacetylation and nucleophilic displacement by various primary amines. Suitably protected amine synthons were used to introduce potentially cross-reactive side chain functionalities. Oligomer synthesis on NovaSyn TG amino resin HL allowed for deprotection to liberate the side chain functional groups without cleavage of the oligomers from solid support.

XRF Analysis

MXRF® analysis was conducted on library resin beads positioned within a 96-well plate. Resin-bound library members and controls were first affixed to XRpro® analytical array plate seals (XRpro Corp., Cambridge, MA) using 96-well plate seals

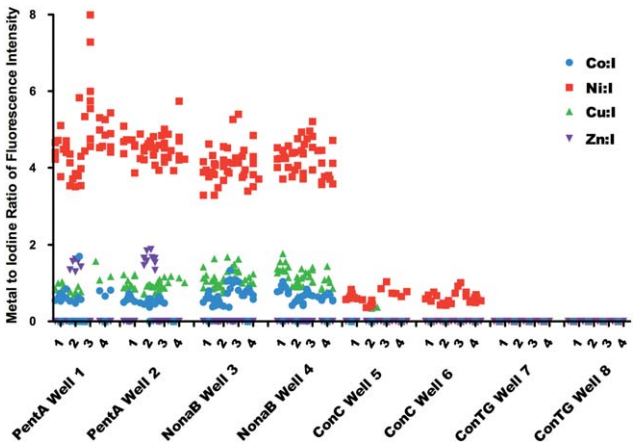

FIGURE 4 Results from the XRF metal-binding screen represented by metal to iodine ratios (M:I) for peptoid sequences **PentA** and **NonaB** and for controls **ConC** and **ConTG** in the presence of four metal species of interest. To demonstrate reproducibility, the designation (1–4) following the sequence and well number denotes different beads bearing identical peptoid sequences. Each sequence was evaluated in two wells within the multi-well plate. The pentamer **PentA** and the nonamer **NonaB** are shown to be capable of selectively complexing Ni^{2+}.

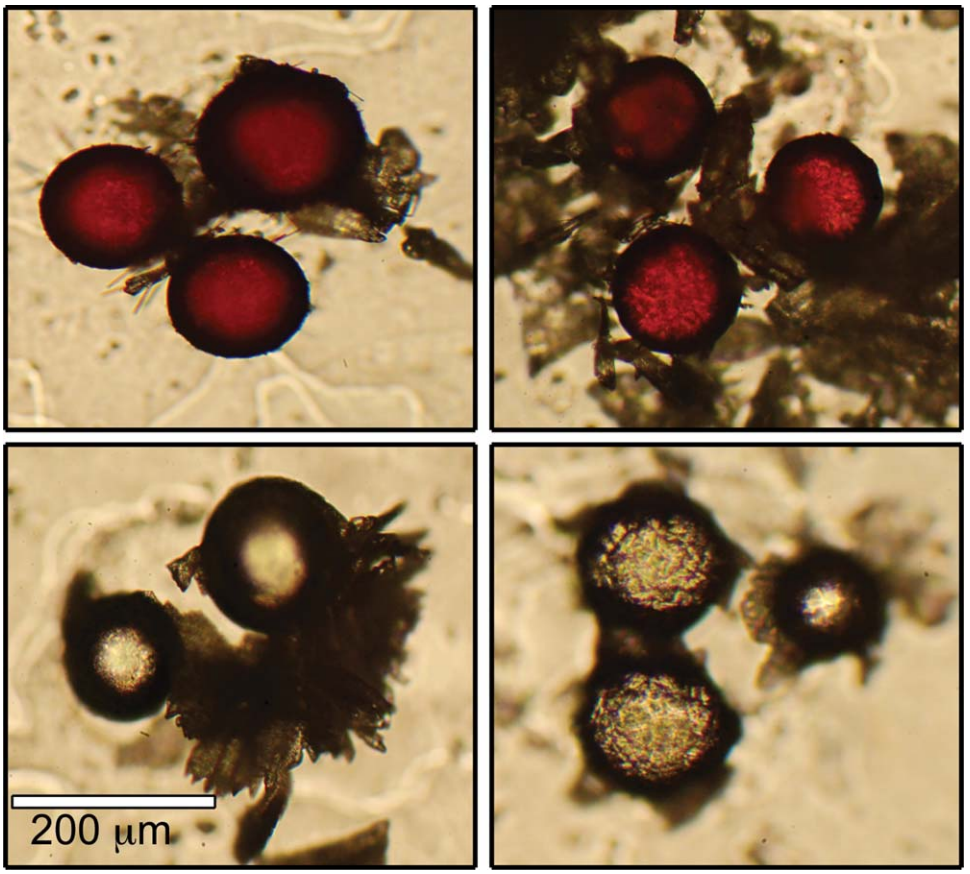

FIGURE 5 Microscope images of peptoids immobilized on TentaGel resin beads after incubation in nickel solution and exposure to 1% dimethylglyoxime solution. A color change to red within the bead matrix indicates binding to nickel. Clockwise from Left: **PentA**, **NonaB**, **ConTG**, **ConC**.

positioning four single-bead samples per well. Two replicate wells were tested for each peptoid sequence. Plate seals were adhered to standard 96-well plates containing a solution of four biologically relevant divalent metal species (Cu^{2+}, Co^{2+}, Ni^{2+}, Zn^{2+}) in aqueous buffer (pH 7) at a concentration of 500 μ*M*/metal. The sealed 96-well plate was inverted so that the solution contacted the resin-bound library, and each peptoid oligomer was incubated separately in the metal mixture prior to MXRF analysis. Following incubation, 10 spectra were acquired for each resin bead using an XRpro® bench-top XRF instrument (XRpro Corp., Cambridge, MA), providing 80 fluorescence spectra per sequence. XRF analysis was conducted through the thin plastic of the XRpro® analytical array plate seal without removing either the plate seal from the 96-well plate or the metal solution from the wells. Background readings were obtained from a position within each well that did not contain a peptoid sample bead, to enable background subtraction of the free metal solution present in each well (10 spectra per well) from the library spectra. This technique was particularly convenient, as it did not require removal of the beads from solution or rinsing protocols. Notably, these 3,600 XRF readings were obtained and recorded in approximately 3 h, an analysis rate of 28,800 readings/day. The experiments were conducted in triplicate against all library members to yield metal binding profiles for each of the oligomers.

Metal-binding peptoid sequences were identified by analyzing the XRF intensity from each of the metals against the signal of the iodine center incorporated within each peptoid oligomer (Metal:Iodine, M:I) (see Supporting Information). These ratios do not indicate precise stoichiometries, and thus, a 1:1 Metal:-Iodine signal does not necessarily correspond to one metal atom bound per peptoid oligomer molecule. However, changes in the ratio for a specific metal can be quantitatively interpreted. For example, a 2:1 Cr:I ratio indicates a twofold greater amount of Cr bound to the peptoid than a 1:1 Cr:I ratio. Therefore, larger M:I ratios indicate better binders, relative to other sequences, and greater differences in the magnitude of M:I among different metals indicate enhanced selectivity for the given metal by the individual sequence. We observed some run-to-run variations in M:I fluorescence signal intensity, but

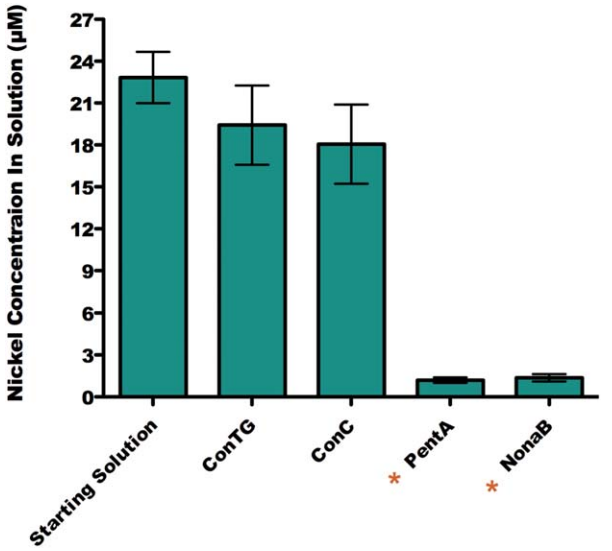

FIGURE 6 Chart of the nickel concentration in solution (μ*M*) before and after exposure to resin beads. From left: Ni concentration of the starting solution; Ni concentration after exposure to control, **ConTG**; control, **ConC**; pentamer, **PentA**; nonamer, **NonaB**. Error bars represent the standard deviation of the experimental results conducted in triplicate. *Indicates concentrations at the ICP-MS detection limit.

overall binding patterns based on relative M:I values for different metal species could be reliably interpreted (see Supporting Information Figures S4.1–4.3).

A subset of peptoids from the library displayed binding capability for most of the metals present. Two peptoid sequences, a pentamer, **PentA**, and a nonamer, **NonaB**, (Figure 3) containing adjacently paired pyridine and carboxylic acid functionalities were found to preferentially bind nickel relative to the other three metals (Figure 4, see Supporting Information Figure S5). In contrast, the two controls (**ConC** and **ConTG**) presented negligible binding activity with all four metals. Notably, one sequence (**NonaD**), which similarly incorporated pyridine and carboxylic acid side chain groups within a different and non-adjacent sequence motif did not exhibit the same strong selectivity for nickel or the large M:I values as observed for **PentA** and **NonaB** (see Supporting Information Figure S4.3). These results indicate that both monomer composition and sequence are important for establishing suitable metal binding environments and also suggest that the proper positioning of multiple metal-complexing side chain types may be required to enable selective binding.

Metal Complexation With Liberated Sequences

Considering the strong response of resin-bound **PentA** and **NonaB** to Ni^{2+}, we anticipated that the liberated oligomers in free solution would participate in nickel complexation upon cleavage from resin. **PentA**, **NonaB**, and **ConC** were re-synthesized on Rink Amide resin, cleaved from solid support, and purified to >90% via reversed-phased high performance liquid chromatography. The identity of the sequences was verified by electrospray ionization mass spectrometry (see Supporting Information). However, binding events between Ni^{2+} and **PentA** or **NonaB** could not be detected in solution (data not shown). Although the chemical composition of the resin-bound and liberated peptoid oligomers bearing C-terminal amides are distinct, the origin of variation in metal binding characteristics by immobilized versus free peptoids is a focus of continuing investigation.

Ni-Dimethylglyoxime Colorimetric Assay

In order to validate the ability of resin-bound **PentA** and **NonaB** to bind Ni(II), a colorimetric on-resin assay with dimethylglyoxime, a competitive chelator for Ni(II), was performed.[28,30,35] In this assay, Ni(II) binding is characterized by a color change to red within the bead matrix. As controls, **ConC** and unmodified Tentagel Beads (**ConTG**) were also analyzed. All resin beads were affixed to XRpro® analytical array plate seals and incubated in standard 96-well plates containing 3 mL of aqueous buffered 500 μ*M* $Ni(NO_3)_2$ for 3 h. Each individual sequence was plated in 12 separate wells. Prior to imaging, the beads were washed with buffer, then exposed to a 1% dimethylglyoxime solution. Relative to **ConC** and **ConTG**, which displayed no color change, **PentA** and **NonaB** appeared bright red (Figure 5). These results confirm that **PentA** and **NonaB** bind Ni(II).

Nickel Depletion Assay

Encouraged by the verification of nickel binding by colorimetric analysis, we sought to quantify the hit oligomers' ability to sequester Ni^{2+} from aqueous solution. Each of the resin-bound oligomers and controls was incubated in two different concentrations of buffered nickel solutions at pH 7. The solutions were then filtered and tested for nickel concentration, relative to the nickel stock solution.

When exposed to 10 mL of a nickel solution at an initial concentration of 24.1 μ$M \pm 1.8$ (0.241 μmol), both **PentA** and **NonaB** (1.95 μmol of each peptoid immobilized on resin, based on loading levels) achieved a dramatic reduction in the nickel concentration (Figure 6). Following incubation for 3 h, the concentration of nickel remaining in solution was less than 0.97 μ$M \pm 0.2$, a value that was near the detection limit of the ICP-MS analysis. This corresponds to an average complexation of 96.0% of the initial Ni^{2+}, after incubation in the presence of **PentA.** Likewise, **NonaB** removed an average of 95.5% of the nickel, leaving

1.1 $\mu M \pm 0.3$ of free Ni^{2+} in solution. In sharp contrast, neither **ConC** nor **ConTG** exhibited comparable capacity to deplete nickel from the same 24 μM starting solution, and their nickel depletion averaged 16.7% and 13.4%, respectively. This behavior is expected for control species lacking suitable functional groups to promote metal complexation. These findings are in agreement with those obtained from the MXRF experiments, indicating that the sequences' affinity for nickel follows the order: **PentA**, **NonaB** >> **ConC** > **ConTG**. An additional depletion assay conducted at ten times the initial concentration of nickel (222.5 $\mu M \pm 22.8$) yielded similar affinity patterns (see Supporting Information Figure S6).

CONCLUSION

We demonstrate the use of high-throughput XRF to screen a library of peptoid oligomers for metal binding interactions in the presence of several, biologically relevant, competing metal ions. Two sequences display strong affinity for Ni(II) relative to the other metals present in solution. Additional metal-binding assays, which include a qualitative colorimetric assay and a quantitative ICP-MS concentration depletion assay, demonstrate the viability of this technique. The application of this approach can be expanded to potentiate the discovery of new "metallopeptoid" sequences capable of performing additional functions. For example, peptoid sequences that preferentially bind specific metals could be elaborated into mimics of metalloprotein catalysts.

The scope of this screening protocol is not limited to the detection of metal-binding interactions.[36] The gain or loss of any atom with an atomic number larger than 12 can be monitored. Hence, the versatility, ease, and speed of this technique indicate that it will be a useful complement to previously established peptoid high-throughput screening methods and will enable the discovery of new families of functional oligomeric materials.[28,32,37,38]

Authors would like to thank Chin Lin, Ronald McLurkin, John Hsieh, and Emilia Solomon for assistance with instrumentation. They also thank Paul Levine for his contributions to the figures. Benjamin Warner and Nathan Zahler are employees of XRpro Corp. and own shares in the parent company of XRpro Corp., Caldera Pharmaceuticals, Inc.

REFERENCES

1. (a) Fowler, S. A.; Blackwell, H. E. Org Biomol Chem 2009, 7, 1508–1524; (b) Sun, J.; Zuckermann, R. N. ACS Nano 2013, 7, 4715–4732; (c) Luxenhofer, R.; Fetsch, C.; Grossmann, A. J Polym Sci A Part A: Polym Chem 2013, 51, 2731–2752; (d) Yoo, B.; Kirshenbaum, K. Curr Opin Chem Biol 2008, 12, 714–721.
2. (a) Figliozzi, G. M.; Goldsmith, R.; Ng, S.; Banville, S. C.; Zuckermann, R. N. Methods Enzymol 1996, 267, 437–447; (b) Culf, A. S.; Oulette, R. J. Molecules 2010, 15, 5282–5335.
3. Zuckermann, R. N.; Martin. E. J.; Spellmeyer, D. C.; Stauber, G. B.; Shoemaker, K. R.; Kerr, J. M.; Figliozzi, G. M.; Goff, D. A.; Siani, M. A.; Simon, R. J.; Banville, S. C.; Brown, E. G.; Wang, L.; Richter, L. S.; Moos, W. H. J Med Chem 1994, 37, 2678–2685.
4. Zuckermann, R. N. Biopolymers 2011, 96, 545–555.
5. Patch, J. A.; Kirshenbaum, K.; Seurynck, S. L.; Zuckermann, R. N.; Barron, A. E. In Pseudo-Peptides in Drug Discovery; Nielsen, P. E., Ed.; Wiley-VCH: Weinheim, 2004; pp 1–31.
6. Huang, C.-Y.; Uno, T.; Murphy, J. E.; Lee, S.; Hamer, J. D.; Escobedo, J. A.; Cohen, F. E.; Radhakrishnan, R.; Dwarki, V.; Zuckermann, R. N. Chem Biol 1998, 5, 345–354.
7. Dohm, M. T.; Seurynck-Servoss, S. L.; Seo, J.; Zuckermann, R. N.; Barron, A. E. Biopolymers 2009, 92, 538–553.
8. Udugamasooriya, D. G.; Dineen, S. P.; Brekken, R. A.; Kodadek, T. J Am Chem Soc 2008, 130, 5744–5752.
9. (a) Paulick, M. G.; Hart, K. M.; Brinner, K. M.; Tjandra, M.; Charych, D. H.; Zuckermann, R. N. J Comb Chem 2006, 8, 417–426; (b) Alluri, P. G.; Reddy, M. M.; Bachhawat-Sikder, K.; Olivos, H. J.; Kodadek, T. J Am Chem Soc 2003, 125, 13995–14004; (c) Lam, K. S.; Salmon, S. E.; Hersh, E. M.; Hruby, V. J.; Kazmierski, W. M.; Knapp, R. J. Nature 1991, 354, 82–84.
10. Chongsiriwatana, N. P.; Patch, J. A.; Czyzewski, A. M.; Dohm, M. T.; Ivankin, A.; Gidalevitz, D.; Zuckermann, R. N.; Barron, A. E. Proc Natl Acad Sci USA 2008, 105, 2794–2799.
11. Huang, M. L.; Benson, M. A.; Shin, S. Y.; Torres, V. J.; Kirshenbaum, K. Eur J Org Chem 2013, 3560–3566.
12. Levine, P. M.; Imberg, K.; Garabedian, M. J.; Kirshenbaum, K. J Am Chem Soc 2012, 134, 6912–6915.
13. Turner, J. P.; Lutz-Rechtin, T.; Moore, K. A.; Rogers, L.; Bhave, O.; Moss, M. A.; Servoss, S. L. ACS Chem Neurosci 2014, 5, 552–558.
14. Maayan, G.; Ward, M.; Kirshenbaum, K. Proc Natl Acad Sci USA 2009, 106, 13679–13684.
15. Della Sala, G.; Nardone, B.; De Riccardis, F.; Izzo, I. Org Biomol Chem 2013, 11, 726–731.
16. Statz, A. R.; Meagher, R. J.; Barron, A. E.; Messersmith, P. B. J Am Chem Soc 2005, 127, 7972–7973.
17. Huang, M.; Ehre, D.; Jiang, Q.; Hu, C.; Kirshenbaum, K.; Ward, M. Proc Natl Acad Sci USA 2012, 109, 19922–19927.
18. Nam, K. T.; Shelby, S. A.; Marciel, A. B.; Choi, P. C.; Chen, R.; Tan, L.; Chu, T. K.; Mesch, R. A.; Lee, B.-C.; Connolly, M. D.; Kisielowski, C.; Zuckermann, R. N. Nat Mater 2010, 9, 454–460.
19. Sanii, B.; Kudirka, R.; Cho, A.; Venkateswaran, N.; Oliver, G. K.; Olson, A. M.; Tran, H.; Harada, R. M.; Tan, L.; Zuckermann, R. N. J Am Chem Soc 2011, 133, 20808–20815.
20. Chen, C. L.; Qi, J.; Zuckermann, R. N.; DeYoreo, J. J. J Am Chem Soc 2011, 133, 5214–5217.
21. Kölmel, D. K.; Rudat, B.; Schepers, U.; Bräse, S. Eur J Org Chem 2013, 2761–2765.
22. Izzo, I.; Ianniello, G.; De Cola, C.; Nardone, B.; Erra, L.; Vaughan, G.; Tedesco, C.; De Riccardis, F. Org Lett 2013, 15, 598–601.
23. Maayan, G.; Ward, M.; Kirshenbaum, K. Chem Commun 2009, 56–58.
24. Lee, B.-C.; Chu, T. K.; Dill, K. A.; Zuckermann, R. N. J Am Chem Soc 2008, 130, 8847–8855.

25. Pirrung, M. C.; Park, K.; Tumey, L. N. J Comb Chem 2002, 4, 329–344.
26. Maayan, G.; Lui, L.-K. Biopolymers 2011, 96, 697–687.
27. De Cola, C.; Fiorillo, G.; Meli, A.; Aime, S.; Gianolio, E.; Izzo, I.; De Riccardis, F. Org Biomol Chem 2014, 12, 424–431.
28. Knight, A. S.; Zhou, E. Y.; Pelton, J. G.; Francis, M. B. J Am Chem Soc 2013, 135, 17488–17493.
29. Fischer, A. E. O.; Naughton, D. P. J Inorg Biochem 2004, 98, 343–346.
30. Francis, M. B.; Finney, N. S.; Jacobsen, E. N. J Am Chem Soc 1996, 118, 8983–8984.
31. X-Ray Data Booklet; Thompson, 3rd ed.; Albert C., Ed.; [Online]; Lawrence Berkeley National Laboratory: Berkeley, California, 2009. Available at: http://xdb.lbl.gov/xdb-new.pdf. Last accessed Apr 20, 2014.
32. Miller, T. C.; Mann, G.; Havrilla, G. J.; Wells, C. A.; Warner, B. P.; Baker, R. T. J Comb Chem 2003, 5, 245–252.
33. Minogue, E. M.; Havrilla, G. J.; Taylor, T. P.; Warner, B. P.; Burrell, A. K. New J Chem 2006, 30, 1145–1148.
34. Burkoth, T. S.; Fafarman, A. T.; Charych, D. H.; Connolly, M. D.; Zuckermann, R. N. J Am Chem Soc 2003, 125, 8841–8845.
35. Godycki, L. E.; Rundle, R. E. Acta Cryst 1953 6, 487–495.
36. (a) Singer, D. M.; Zachara, J. M.; Brown Jr, G. E. Environ Sci Technol 2009, 43, 630–636; (b) Janssens, K.; Vittiglio, G.; Deraedt, I.; Aerts, A.; Vekemans, B.; Vincze, L.; Wei, F.; Deryck, I.; Schalm, O.; Adams, F.; Rindby, A.; Knöchel, A.; Simionovici, A.; Snigirev, A. X-ray Spectrom 2000, 29, 73–91; (c) Buleon, A.; Cotte, M.; Putaux, J. L.; d'Hulst, C.; Susini, J. Biochem Biophys Acta 2014, 1840, 113–119; (d) Grubman, A.; James, S. A.; James, J.; Duncan, C.; Volitakis, I.; Hickey, J. L. Crouch, P. J.; Donnelly, P. S.; Kanninen, K. M.; Liddell, J. R.; Cotman, S. L.; de Jonge, M. D.; White, A. R. Chem Sci, 2014, 5, 2503–2516.
37. Sambasivan, R.; Zheng, W.; Burya, S. J.; Popp, B. V.; Turro, C.; Clementi, C.; Ball, Z. T. Chem Sci, 2014, 5, 1401–1407.
38. Stanton, M. L.; Holcombe, J. A. J Comb Chem 2007, 9, 359–365.